Pergamon

Planet. Space Sci., Vol. 46, No. 9/10, pp. 1291–1304, 1998

0032–0633/98/$—see front matter

PII: S0032–0633(98)00025–7

VIRTIS: an imaging spectrometer for the ROSETTA mission

A. Coradini[1], F. Capaccioni[1], P. Drossart[2], A. Semery[2], G. Arnold[3], U. Schade[3], F. Angrilli[5], M. A. Barucci[2], G. Bellucci[4], G. Bianchini[5], J. P. Bibring[10], A. Blanco[6], M. Blecka[15], D. Bockelee-Morvan[2], R. Bonsignori[8], M. Bouye[2], E. Bussoletti[7], M. T. Capria[1], R. Carlson[16], U. Carsenty[3], P. Cerroni[1], L. Colangeli[7], M. Combes[2], M. Combi[12], J. Crovisier[2], M. Dami[8], M. C. DeSanctis[1], A. M. DiLellis[4], E. Dotto[1], T. Encrenaz[2], E. Epifani[6], S. Erard[10], S. Espinasse[1], A. Fave[1], C. Federico[17], U. Fink[14], S. Fonti[6], V. Formisano[4], Y. Hello[2], H. Hirsch[3], G. Huntzinger[1], R. Knoll[2], D. Kouach[2], W. H. Ip[18], P. Irwin[19], J. Kachlicki[3], Y. Langevin[10], G. Magni[1], T. McCord[13], V. Mennella[7], H. Michaelis[3], G. Mondello[8], S. Mottola[3], G. Neukum[3], V. Orofino[6], R. Orosei[1], P. Palumbo[7], G. Peter[3], B. Pforte[1], G. Piccioni[4], J. M. Reess[1], E. Ress[3], B. Saggin[5], B. Schmitt[11], D. Stefanovitch[2], A. Stern[20], F. Taylor[19], D. Tiphene[2], G. Tozzi[9]

[1] Istituto di Astrofisica Spaziale CNR, Viale dell'Università 11, 00185 Rome, Italy
[2] Observatoire de Paris Section de Meudon, France
[3] Istitut Für Planeterkundung DLR—Berlin, Germany
[4] Instituto di Fisica dello Spazio Interplanetario CNR, Italy
[5] Dipartimento di Ingegneria Meccanica, Università di Padova
[6] Dipartimento di Fisica, Università di Lecce, Italy
[7] Osservatorio Astronomico di Capodimonte, Naples, Italy
[8] Officine Galileo—Florence, Italy
[9] Osservatorio Astrofisico di Arcetri, Florence, Italy
[10] Institut d'Astrophysique Spatial CNRS, Orsay, France
[11] Laboratorie de Glaciologie et Geophysique de l'Environment, Grenoble, France
[12] Space Physics Research Laboratory, University of Michigan, Ann Arbor, U.S.A.
[13] Hawaii Institute of Geophysics and Planetology, University of Hawaii, Honolulu, U.S.A.
[14] Luna Planetary Laboratory, University of Arizona, Tucson, U.S.A.
[15] Polish Academy of Sciences, Warsaw, Poland
[16] NASA JPL, Pasadena, U.S.A.
[17] Università di Perugia, Italy
[18] MPI—Katlenburg, Germany
[19] Atmospheric, Oceanic and Planetary Physics Department, Oxford University, U.K.
[20] Southern Research Institute, Boulder, U.S.A.

Received 15 April 1997; revised 12 January 1998; accepted 19 January 1998

Abstract. The VIRTIS scientific and technical teams will take advantage of their previous experience in the design and development of spectrometers for space applications. In fact, the various groups contributing to the VIRTIS experiment, from Italy, France and Germany, have been deeply involved in the CASSINI mission, with the experiments VIMS and CIRS. The targets of the ROSETTA mission are the most primitive solar system bodies: comets and asteroids. ROSETTA will study in detail a comet nucleus, the prime target of the mission, and will fly by one or two asteroids. The small bodies of the solar system are of great interest for planetary science and their study is crucial to understand the solar system formation. In fact it is believed that comets and, to a lesser extent, asteroids underwent a moderate evolution so that they preserve some pristine solar system material. Comets and asteroids are in close relationship with the planetesimals, which formed from the solar nebula 4.6 billion years ago. The global characterisation of one comet nucleus and one or two asteroids will provide basic information on the origin of the solar system and on the interrelation between the solar system and the interstellar dust environment.

The ROSETTA mission is designed to obtain the above mentioned scientific goals by: (a) *in situ* analysis of comet material; (b) long period of remote sensing of the comet. The combination of remote sensing and *in situ* measurements will increase the scientific return of the mission. In fact, the "*in situ*" measurements will give relevant "ground-truth" for the remote sensing

Correspondence to: A. Coradini

information, and, in turn, the locally collected data will be interpreted in the appropriate scenario provided by remote sensing investigation. The scientific payload of ROSETTA includes a Visual InfraRed Spectral and Thermal Spectrometer (VIRTIS) among the instrument on board the spacecraft orbiting around the comet.

This instrument is fundamental to detect and study the evolution of specific fingerprints—such as the typical spectral bands of minerals and molecules—arising from surface components and from materials dispersed in the coma. Their identification is a primary goal of the ROSETTA mission as it will allow us to identify the nature of the main constituent of the comets. Moreover, the surface thermal evolution during comet approach to Sun is important information that can be obtained by means of spectroscopic observation. The VIRTIS design and its detailed science goals are reported hereafter.

Introduction

Comets are a heterogeneous class of objects as they accreted in the region spanning from Jupiter to Neptune or beyond, where the thermodynamical conditions were greatly non-homogeneous at the time of the solar system formation. (Rickman and Huebner, 1990). Comets are believed to be the most primitive objects in the solar system, because they have spent their life in a cold environment and are unlikely to be thermally altered. Only collision mechanisms can be responsible for an extensive resurfacing and, in many cases, for a collisional evolution (Farinella and Davis 1996). When a comet enters the inner solar system a coma is formed by the sublimation of ices, followed by dust ejection and differentiation of the subsurface layers.

On the basis of present knowledge, a comet nucleus is an irregularly shaped object, containing heterogeneous mixture of ices and dust, with variable surface albedo, composition and thermal properties. The spatial and temporal irregularity of the nucleus activity leads to a non-uniform surface, with topographic features and roughness at different scales. The accretion of the nucleus by collisions between grains may occur at low temperatures and low relative velocities (order of 1–10 m/s). This mechanism can produce a highly porous and loose aggregate with no tendency to subsequent compression due to very small gravitational forces. On the other hand, the thermal evolution of the nucleus, in the inner solar system, determines the sublimitation of ices and their successive re-condensation in colder regions, causing reduction of the pore sizes and an increase of the material strength (Haruyama *et al.*, 1993). The comet dust and gas production was found to come from a limited number of discrete sources, with the rest of the surface almost completely inactive (Keller *et al.*, 1988). The surface of P/Halley is a clear example: it is heterogeneous and displays two different units. The first is dominated by brighter, possibly unaltered materials, which could be interpreted as ices. The second is characterised by darker, probably altered assemblies such as complex organic and secondary inorganic (Keller *et al.*, 1988). The abundance of volatile elements suggests that the related ices and gases may be primordial. The nature of the solid compounds of the comets (silicates, oxides, salts, organics and ices) is still unknown. These chemical compounds can be identified by infrared spectroscopy using high spatial resolution imaging to map the heterogeneous parts of a nucleus and high spectral resolution spectroscopy to determine the composition unambiguously.

The visual and infrared spectrum of the comet coma is characterised by a number of components comprising both gas emission bands and a dust continuum (Bockelee-Morvan and Crovisier, 1992). Ground-based visual spectroscopy has detected various atomic, radical and ionic species formed through photo-dissociation by solar ultraviolet radiation of the so-called "parent" molecules which are sublimated from the nucleus and possibly from a halo of volatile grains. Previous IR comet observations have shown that various hydrocarbons show emission bands between 3 and 4 μm.

Scientific objectives

The ROSETTA mission is devoted to the detailed study of a comet nucleus and two main belt asteroids.

A Multispectral Imager—covering the range from the near UV (0.25 μm) to the near IR (5.0 μm) and having moderate to high spectral resolution and imaging capabilities—is an appropriate instrument for the determination of the comet global (size, shape, albedo, etc.), and local (mineralogical features, topography, roughness, dust and gas production rates, etc.) properties.

The main scientific objectives of the ROSETTA-VIRTIS instrument will be achieved through a combination of the high spatial resolution channels (-M) and a high spectral resolution channel (-H). These objectives are: (1) to determine the nature of the solids on the nucleus surface (composition of ices, dust and characterisation of organic compounds); (2) to identify the gaseous species; (3) to monitor the gaseous activity, and its spatial distribution; (4) to characterise the physical conditions of the coma, to measure the temperature of the nucleus; (5) to help the selection of the landing sites and to give support for other instruments.

In the present ROSETTA mission scenario, the target, is comet P/Wirtanen. This comet was discovered in 1948 (Wirtanen, 1948) and its orbit had, at that time, an inclination of 13°, a perihelion distance of 1.6 AU and a period of 6.7 years, typical of a Jupiter family object. Its chaotic orbit is often perturbed by close encounters with Jupiter, as happened in 1972 and 1984: currently the period is 5.8 years, the perihelion distance 1.06 AU and the aphelion distance 5.3 AU, and according to Carusi *et al.* (1995), the orbital parameters in the 2000 will not vary appreciably.

The comet has been poorly observed until its last perihelion passage on 14 March 1997. Apart from the astrometric positions, the only data published were visual magnitudes estimated by amateurs and photographic photometry of the Schmidt plates used for the comet discovery in 1948 and recoveries in 1954, 1960, 1974 and

1985 (Schulz and Schwehm, 1996). From visual lightcurves, Jorda and Rickman (1995) estimated a water production rate of 4×10^{28} molecules/s at perihelion. They also found indications of a possible bright flare of one magnitude in 1986. From photographic observations it is possible to estimate an absolute visual magnitude of 16.5. On the basis of the visual magnitude of the nucleus and of the lightcurves, if a geometric albedo of 0.03 is assumed, a P/Wirtanen radius of less than 2 km was deduced (Schulz and Schwehm, 1996). A'Hearn *et al.* (1997), on the basis of accurate statistics of different comets and taking into account the localised activity, have estimated the maximum emission rate of P/Wirtanen at the perihelion to be about 10^{28} molecules/s.

Recent observations of comet P/Wirtanen have provided new constraints on the production rate: water production rate of 7×10^{27} molecules/s has been measured, by SWAN experiment on board the SOHO spacecraft (Bertaux, pers. commun.). Several papers containing estimations of P/Wirtanen activity derived from thermal evolution and differentiation models of the nucleus have been published (Capria *et al.*, 1996; Podolak and Prialnik, 1996; Benkhoff and Boice, 1996). These models are still preliminary and will be updated when the observational results of the 1996/1997 Wirtanen observation campaign are available, but it is already known that the order of magnitude of the comet model parameters are correct.

Comet nucleus

One of the main goals of ROSETTA mission will be the determination of the global characteristics of the nucleus. On the basis of the present knowledge and models, the upper layer is expected to be partly or even completely depleted due to ice sublimation: however the presence on the surface of localised ice-rich areas cannot be excluded. A reasonable analogue of a comet reflectance properties in the visible range–IR could be a mixture of ice, aged snow and dust. The reflectance of the comet surface is expected to be very low. *In situ* GIOTTO observations show an albedo of 0.04 of comet Halley (Keller *et al.*, 1988). The comet composition is such that the comet will be very dark (albedo <0.1) (A'Hearn *et al.*, 1997). Considerable reduction of reflectivity of pure ice is achieved even with very small amounts of inclusions: the pure snow reflectivity which, in the visible, is approximately 0.9, can be reduced to less than 0.3 with a dust to ice mass ratio of only 10^{-3} (Clark, 1981).

The most abundant species are H_2O (more than 80%), CO, CH_3OH, and CO_2, H_2CO (NH_3 being less abundant). As on P/Halley, we expect to find inactive surfaces and strongly localised outgassing activity. The inactive areas are probably covered with a regolith of small-size particles, the active area may be characterised by the presence of ice processed during the earlier heating periods. These areas are evolving with time, and possibly will change their properties during the ROSETTA mission. Radiation processes may have altered the primary mineral phases, as well as the ices (H_2O, CH_3OH, etc.). Simple hydrocarbons could have been polymerised and gas-solid processes could have altered primary silicates. Secondary phyllosilicates Fe-oxides (magnetite) and some salts may have been formed. All these elements should be searched for. Only the inner frozen nucleus should contain unaltered chondritic component.

Table 1. Main mineralogic bands in the near infrared

Species	Diagnostic features (μm)
Ferric/ferrous minerals	0.8–2.0
Olivine	Triplets of bands around 1.0 (0.86, 1.06, 1.33)
Pyroxenes	0.8–1.0, 1.8–2.35
Hydrated minerals	1.4, 1.9, 2.9–3.3
Clay minerals and others	1.4, 1.9, 2.16–2.23
Phyllosilicates	ca 2.3
Carbonates	Set of features 2.0–3.3 and near 4.5
Magnetite	Bands at 0.6–0.9

The spectral characteristics of comet nuclei are likely to show features linked with the minerological composition and presence of ices. The wavelength range of VIRTIS from 0.25 up to 5 μm is diagnostic for ices, minerals and organic compounds. Moreover within a distance of 3 AU from the Sun the long wavelength part of the spectrum can be used to study the comet surface temperatures. Global mapping of the nucleus will provide important information about the distribution of minerals, inorganic and organic ices (-M). The exact identification of organic material requires a spectral resolving power above 1000. For this objective observation of -M will be supported by -H channel. Temperature distribution and temperature monitoring of active and inactive areas compared with the spectral albedo maps and gas production will allow the study of the thermal properties and thermal balance of the nucleus and to infer the comet subsurface composition. An inventory of the main topographic features will help clarify the geological history and the evolution of the comet. In fact these bodies receive most of their energy from the outside, and their geological history is strongly related to their thermal history and to their topography (Coradini *et al.*, 1997a, b).

Minerals that are expected to be found on the comet surface are reported in Table 1. Secondary minerals, such as phyllosilicates, have water and OH absorption features in the 2.9–3.3 μm range, and at 1.4 and 1.9 μm. The presence of the 1.4 and 1.9 μm bands is indicative of undissociated water in the mineral, while the presence of the 1.4 μm band alone suggests OH groups like hydroxyls. The exact position of these bands should be diagnostic of the mineralogy of the comet. Several absorption bands of water-ice fall in the near infrared (Table 2). Other ices, like NH_3, CO_2 or H_2S can also be identified by their typical spectral features.

Figure 1 shows laboratory spectra of hydrocarbon ices (C_2H_2, C_2H_4, C_2H_6, C_3H_8, CH_4). A global mapping of the nucleus at these wavelengths will give important information on the surface mineralogy, on the molecular compositions of organic compounds in the mantle and on the presence of ices.

These observation will provide an accurate measure of the dust and gas production rate from localised activity

Table 2. Major absorption bands of inorganic ices from 1 to 5 microns

Species						
H_2O	3.11 (ν_3)	2.94	2.0	1.60	1.25	1.04
CO_2	4.26 (ν_3)	3.33	2.70	2.02		
CH_4	3.32 (ν_3)	2.60	2.33	1.72		
CO	4.68 (ν_1)	2.34	1.56			
NH_3	2.96 (ν_1)	2.28	2.00	1.65	1.52	
H_2S	3.94 (ν_1, ν_3)	2.70	2.04			
SO_2		4.37	4.07	3.77		
N_2	4.24 (ν_1)	2.15				

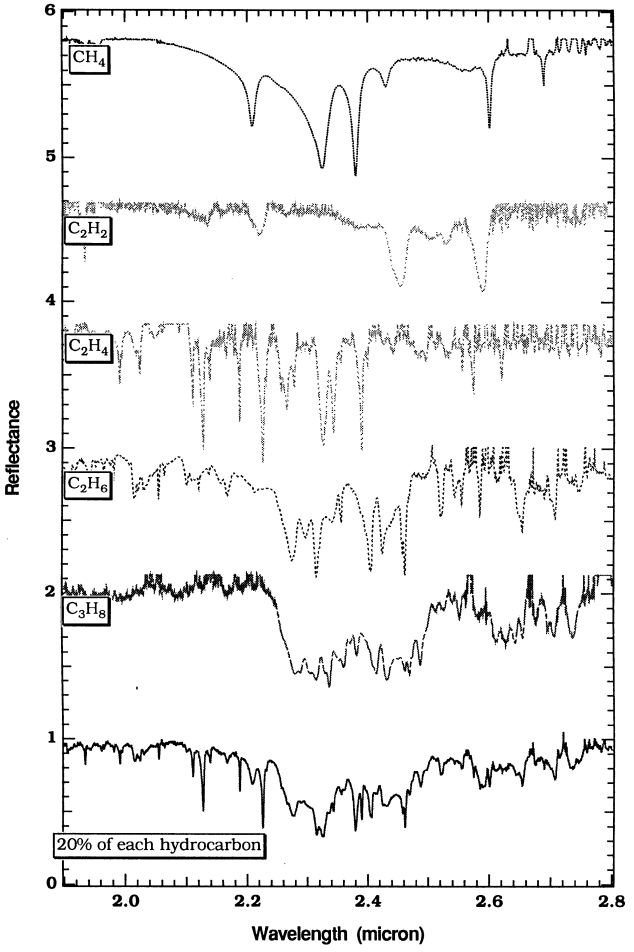

Fig. 1. Reflectance spectra of 5 different solid hydrocarbons and a mixture of them (20% each) at a resolving power of 1500–2500. Grain size used: 5 μm. The aim is to show that at a high spectral resolution, it is possible to identify specific bands of a molecule in a complex mixture of several molecules of the same chemical family

regions, thus providing some knowledge of the comet subsurface composition and a map of active regions.

Coma

When the comet enters the inner solar system, the volatiles are released to form a transient atmosphere around the nuclei. Ground based spectroscopy provided the identification of various atomic and molecular species (Table 3).

The optical spectra of comets are characterised by emissions from radicals and ions, while the infrared part of the spectra is more useful for the direct investigations of molecules (Bocklee-Morvan and Crovisier, 1992). The *in situ* analysis of comet activity could give information on controversial topics concerning the formation and composition of a comet atmosphere. The VIRTIS instrument can make an extremely valuable contribution to the coma science. Its extensive wavelength coverage, over more than four spectral octaves from 0.25 to 5.0 μm, means that many different types of molecules can be investigated, from the strong 0.29 μm UV OH emission to the 4.7 μm fundamental CO band. Essentially, all the fundamental bands of important expected molecules are covered. This large spectral range coupled with good spectral resolution is combined with the excellent spatial resolution required for the investigation of many of the near nucleus phenomena. A considerable enhancement for the coma science is furthermore obtained by combining the spot measurements of the high spectral resolution channel -H with the spatial resolution and field of view of the lower spectral resolution channel -M.

Thanks to spectroscopic ground-based and space-borne observations, quantitative detection of various volatiles has been possible: H_2O, CO_2, H_2CO, CH_3OH, H_2S, HCN, CO and CH_4. It has been also shown that atoms, radicals, and ions, not expected to be produced directly from the nucleus, are important constituents of comet coma (Festou *et al.*, 1986). The formation of such species results from the photolysis of the parent molecules initially incorporated in the ice and/or in the grains, and subsequent phase reactions. Past IR comet observations have shown that various hydrocarbons, not fully identified, but possibly Polycyclic Aromatic Hydrocarbons, PAH) show emission bands between 3 and 4 μm (Combes *et al.*, 1986). Apart from CH_3OH and possibly H_2CO, other molecules ranging from small to large or even possibly grains, have to be present in the spectrum. Figure 2 shows a synthetic spectrum of several gases calculated both for the medium spectral resolution channel -M and high spectral resolution channel -H.

The spectral region 2.6–2.9 μm will be extremely useful to study the thermodynamics of the coma. In fact, in this region are present a number of roto-vibrational bands of water (ν_1, ν_3 fundamental bands and several hot bands). The inversion of the spectrum by means of numerical models of fluorescence excitation and radiative transfer for the water bands in this spectral region will allow retrieval of the water rotational temperature, T_{rot}, as well as the water *ortho*-to-*para* ratio, OPR (Crovisier *et al.*, 1996, 1997). The knowledge of T_{rot} coupled with the results of hydrodynamical model of the cometary atmosphere expansion provides information on the thermodynamical conditions inside the coma. On the other hand, the relative abundance of the *ortho* and *para* nuclear spin species of comet water cannot be modified either by radiative processes or by collision, but is believed to be determined mainly by the temperature at which water was last equilibrated, giving an indication of the primordial stages of cometary formation (Mumma *et al.*, 1987).

Table 3. Fundamental bands of potential comet molecules in the 2.5–5 μm region

σ (cm^{-1})	λ (μm)	Band	g-factor (s^{-1})	Molecule	σ (cm^{-1})	λ (μm)	Band	g factor (s^{-1})	Molecule
2062.2	4.849	v_3	2.5×10^{-3}	OCS	3017.0	3.315	v_4	5.5×10^{-4}	CH_3D
2077.0	4.815	v_3	2.0×10^{-5}	HC_3N	3019.5	3.312	v_3	4.0×10^{-4}	CH_4
2138.0	4.677	v_3	2.3×10^{-5}	CH_3CCH	3047.9	3.281	v_{12}	2.0×10^{-4}	C_6H_6
2143.2	4.666	1–0	2.6×10^{-4}	CO	3105.3	3.220	v_9	1.4×10^{-4}	CH_2CH_2
2157.8	4.634	v_3	2.2×10^{-5}	C_2N_2	3212.9	3.112	v_1	6.2×10^{-4}	H_2O+
2200.0	4.545	v_2	2.2×10^{-5}	CH_3D	3259.0	3.068	v_3	2.4×10^{-3}	H_2O+
2272.0	4.401	v_2	1.1×10^{-4}	HC_3N	3294.8	3.035	v_3	1.7×10^{-4}	CHCH
2289.9	4.367	v_3	1.0×10^{-2}	OC_3O	3311.5	3.020	v_3	3.5×10^{-4}	HCN
2349.1	4.257	v_3	2.6×10^{-3}	CO_2	3327.0	3.006	v_1	8.6×10^{-4}	HC_3N
2727.0	3.667	v_1	6.5×10^{-5}	HDO	3333.7	3.000	v_4	1.5×10^{-4}	HCCCCH
2782.5	3.594	v_1	3.9×10^{-4}	H_2CO	3335.1	2.998	v_1	2.5×10^{-4}	CH_3CCH
2843.3	3.517	v_5	4.6×10^{-4}	H_2CO	3337.0	2.997	v_1	3.4×10^{-5}	NH_3
2844.0	3.516	v_3	1.5×10^{-4}	CH_3OH	3444.0	2.904	v_3	2.0×10^{-5}	NH_3
2901.0	3.447	v_3	4.7×10^{-4}	CH_3CH_2OH	3519.4	2.841	v_3	5.8×10^{-3}	H_3O+
2941.0	3.400	v_2	1.0×10^{-4}	CH_3CCH	3568.0	2.803	1–0	6.0×10^{-5}	OH
2942.0	3.399	v_2	1.9×10^{-4}	HCOOH	3569.0	2.802	v_1	3.6×10^{-4}	HCOOH
2945.0	3.396	v_1	3.3×10^{-5}	CH_3D	3607.0	2.772	v_1	1.0×10^{-4}	H_2O_2
2954.0	3.385	v_1	1.5×10^{-5}	CH_3CN	3608.0	2.772	v_5	6.0×10^{-4}	H_2O_2
2970.0	3.367	v_9	3.5×10^{-4}	CH_3OH	3657.0	2.734	v_1	1.8×10^{-5}	H_2O
2971.0	3.366	v_2	3.9×10^{-4}	CH_3CH_2OH	3660.0	2.732	v_1	1.0×10^{-4}	CH_3CH_2OH
2980.9	3.355	v_6	8.5×10^{-5}	CH_3CCH	3681.0	2.717	v_1	1.3×10^{-4}	CH_3OH
2988.6	3.346	v_{11}	7.3×10^{-5}	CH_2CH_2	3707.0	2.698	v_3	1.9×10^{-4}	HDO
2999.0	3.334	v_2	1.9×10^{-4}	CH_3OH	3755.9	2.662	v_3	2.6×10^{-4}	H_2O

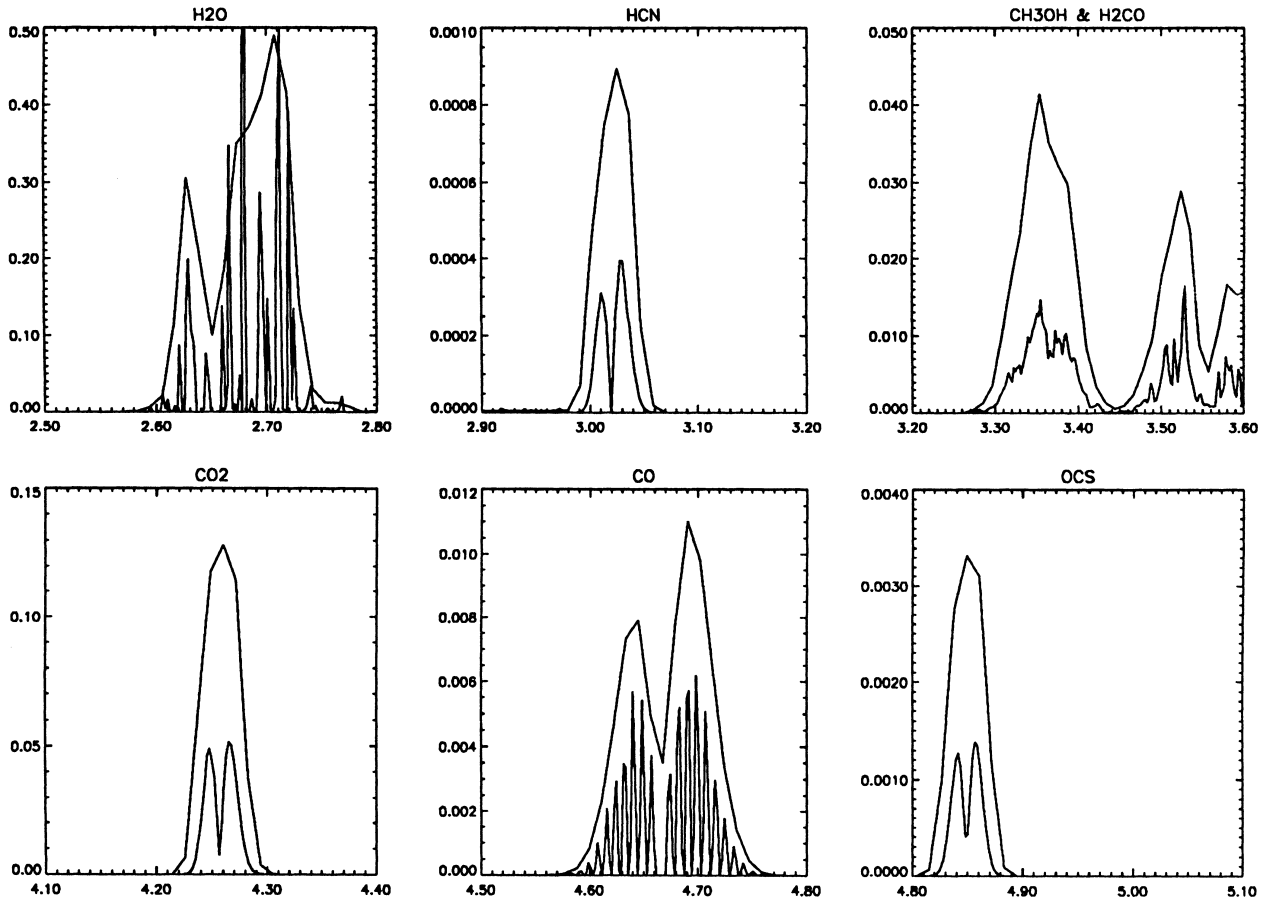

Fig. 2. Synthetic spectra of fluorescence emission (optically thin case) for the spectral resolution of -M (upper curve, multiplied by a constant factor) and -H (lower curve) for H_2O (100%), HCN (0.1%), CH_3OH (5%), H_2CO (1%), CO_2 (3%), CO (5%) and OCS (0.1%)

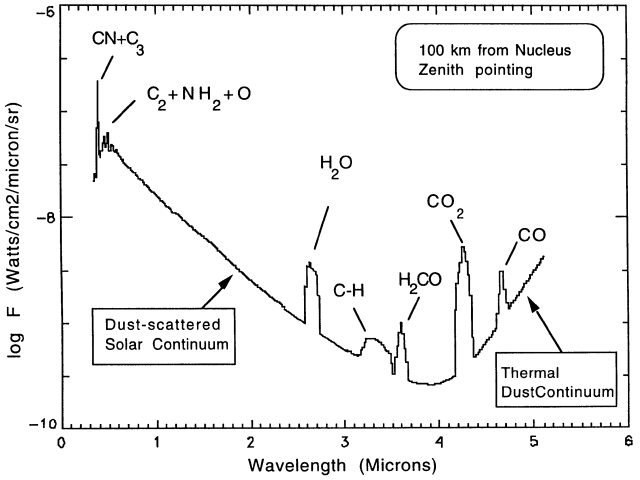

Fig. 3. Synthetic Vis-IR spectrum of the coma. The coma model produces a synthetic spectrum of the target comet at 1.5 AU for the spacecraft positioned at 100 km from the nucleus and pointed in the opposite direction from the nucleus. The model includes contributions from the major gas species and their daughter radicals as well as the continuum contributions from solar radiation scattered from dust particles at short wavelengths and the thermal emission from dust at long wavelengths

Another capability of the high spectral resolution channel is the detection of isotopic species, such as ^{13}CO, $H_2\,^{17}O$, $H_2\,^{18}O$ or HDO with long integration times.

Thanks to the VIRTIS spectral coverage in the visible and UV it will be possible to detect the important emissions of OH (0.28 and 0.31 μm), the main water dissociation product and CN in addition to those of C_3, NH, CH and CO^+.

In the optical region the emission of the comet ions could be observed: CH^+, CO^+, H_2O^+, N_2^+. These ions are the productions of several ionisation mechanisms, and the production rate is related to the Sun direction, the solar wind conditions, and solar field radiation.

In the optical part of the comet spectrum various emission features of the neutral radicals CN, C_2 and NH_2 can be detected. The spectrum contains, possibly, the emissions of $O(^1D)$, a feature associated with the dissociation of water, and the water ion H_2O^+.

The 1–5 μm region is useful for investigations of molecules, because resonant fluorescent excitation is efficient there. The spectrum consists of emission bands superimposed on a background continuum. The strongest feature is the band of H_2O at 2.7 μm. The water is the dominant volatile species of comets (Combes *et al.*, 1986).

The infrared portion of the spectrum is rich in fundamental rotovibrational emissions of a number of important parent molecules: H_2O, CO_2, H_2CO, CH_3OH, CO etc. Table 3 provides a list of possible and expected spectral features of likely gases to be seen in the coma. Figure 3 shows a simulated spectrum of the target comet coma in one pixel of the moderate spectral resolution-mapping channel.

Condensed molecules in the grains ejected in the coma can be studied in the solar reflected spectrum and in emission. The observations of absorption features due to light scattering by organic particles will be difficult. Above 3 μm, where the strong bands of these particles arise, the spectrum is dominated by the emission near perihelion while at larger distances the number density of particles is strongly reduced. The main possibility for the observation of grains is therefore in emission features of fundamental bands, i.e., as for gaseous compounds, above 2.5 μm. Below 5 μm, at least one band of most of the known or suspected comet molecules can be detected, except for the heaviest like SO_2 or S_2. This will permit the identification of the type of bond (chemical family), and possibly the individual molecules for the simpler ones.

New results in comet science

Two new comets C/1996 B2 (Hyakutake) and C/1995 O1 (Hale–Bopp) have approached the Earth in 1996 and 1997. Their observation has produced a huge amount of new data for comet physics. In particular, new species have been detected in the coma, which were unidentified or at most only previously suspected, like C_2H_6 (Mumma *et al.*, 1996) and C_2H_2 (Brooke *et al.*, 1996).

Observations of Hale–Bopp with ISO satellite (Crovisier *et al.*, 1996, 1997) have also provided important pieces of information on comet nuclei. Ten-micron emissions give evidences indicative of crystalline silicate, enriched in magnesium. In the 2.5–5 μm range, ISO/Phot-S observations show early CO_2 emission, when the comets were still at 4.6 AU from the Sun. CO_2 could therefore be detected early in the coma, in addition to CO and H_2O emissions. Observations with ISO/SWS at a spectral resolution of 1500, similar to the VIRTIS-H resolution give the rotational structure of the H_2O band at 2.7 μm, with temperature measurement $T_{rot} = 28.5$ L, and an *ortho/para* ratio of 2.45, suggesting that comet H_2O molecules were formed at low temperature (Crovisier *et al.*, 1997).

Asteroid surface characterisation

Asteroids surface mineralogy and petrology can be studied by means of visible and infrared spectroscopy. Furthermore, the analysis of the spectrophotometric phase curves will give information on surface structures, microroughness and porosity of the surface layers of the target asteroid. As discussed in detail above, for comets, the infrared range contains a wealth of diagnostic spectral features but it is basically unexplored in the study of asteroid surface composition. Several molecular species found in meteorites also produce important visible and near infrared absorption features. Among them, water, OH bearing minerals, carbonates and hydrocarbons are also possibly found on asteroid surfaces. Water-ice itself could be present on some nearest asteroids, recently suggested for Ceres. Instead of the relatively narrow band of ice, however, a broad absorption band has been seen in the spectra of some asteroids and it was interpreted as indicative of the presence of hydrated silicates (Jones *et al.*, 1990). Table 4 summarises the spectral signatures diagnostic for the asteroid surface composition. The high spectral resolution provided by the -H channel could contribute to asteroid studies by delineating subtle absorption features and by refining the measurement of differences in

Table 4. Spectral signatures of mineralogical compounds suspected on asteroids

Species	Features (μm)	Species	Features (μm)
Oxides	0.85–0.89–2.30	Feldspar	1.25
Olivine	1.02–1.05	Phyllosilicates	2.2 (Al–OH)
Ammon. min.	3.0		2.3 (Mg–OH)
Pyroxenes:		Carbonates	2.0–3.3 and $\sim$4.5
Hedenbergite	0.7–0.9	Sulfates	4.2
Augite	0.8	Hydrocarbons C-H	3.4
Enstatite	0.9–1.85	C-N	2.2
Bronzite	0.9–1.80	H_2O Ice	1.4–1.6
Hyperstene	0.9–1.79		2.0 and near 3.0
Pigeonite	1.0	OH and H_2O	3.0
Diopside	1.03–2.3	NH_4-bearing Saponite	3.07

spectral shape. Medium resolution spectral images in the visible and infrared ranges by -M channel will give important information on the mineralogical composition of the target asteroid surface. Spectral resolution added to spatial resolution is needed to identify mineralogical provinces on the asteroid surface.

Scientific requirements and required activity in the different mission phases

A summary of the scientific requirements needed to define the characteristics of VIRTIS is given hereafter.

Nucleus science objectives

- Identification of different ices and ice mixtures and determination of their spatial distribution. This must be done in spite of the very low albedo (<0.1), due to dark inclusions present in the ice and the resulting weak ice spectral features. It must also be done at large distances from the Sun during some phases of the mission.
- Identification of the carbonaceous materials that are probably mixed with water ice, even in low percentages ($<20\%$). The associated spectral features will be very subdued and their identification, from their shape and centre, will require S/N (>100). It will be important also to determine the overall continuum slopes of the spectra, for the presence of organic compounds will redden the spectra in diagnostic ways between 0.4 and 1.1 μm and into the IR as well.
- Determination of the physical microstructure and nature of the surface grains by measuring the spectrophotometric phase curve with a relative radiometric accuracy of about 1%.
- Identification of the silicates, hydrates and other minerals which are expected to be found. Strong but broad absorption features ($\lambda/\Delta\lambda < 20$) should be observed from the visible (0.25–1.0 μm) to the near IR (1.0–5.0 μm), so a spectral resolution of 100 is adequate.
- Determination of the spatial distribution of the various mineralogical types of their mixtures using both the spectral features and the overall brightness. Local fluctuations of the reflectivity and spectral features related to small scale compositional differences are expected. For global mapping of the nucleus, a spatial resolution of a few tens of metres is needed.
- Detection and monitoring of active areas on the comet surface (gas volcanism) to understand the physical processes operating and to identify the material types associated.
- Determination of the composition of ices on the nucleus surface. With the exception of H_2O, condensed molecules display diagnostic narrow (as well as broad) absorption bands in the reflected component (1–3 μm). S/N higher than 100 and a minimum resolving power of 1000 is needed to resolve the bands fully. The -H FOV must be within the field of view of one -M frame (accuracy of few arcminutes) to allow combined operation at both high spatial and spectral resolution.

Coma science objectives

- Determination of the global distribution of gas and dust in the inner coma. Radiometric accuracy of 10% absolute and 1% relative with a resolving power of 100 are required.
- Determination of the dust thermal properties.
- Identification and mapping of the storm molecular emissions in the near ultraviolet and visible portions of the spectrum. These include the main water dissociation product OH (0.28 and 0.31 μm), CN, C_3, NH, CH and CO^+ ions, and the neutral radicals CN and C_2. The combination of high spatial resolution with moderate spectral resolution ($\lambda/\Delta\lambda < 500$) will allow correlation of the evolution of radicals with that of their parent molecules.
- Comparison of the results of these measurements with ground based telescopic observations.
- Mapping of the composition and evolution of gas and dust jets in the coma and comparison with the mineralogical composition and spatial morphology of active regions on the surface of the nucleus.
- Determination of the composition of the dust grains in the coma by observing emission features in the fundamental bands between 2.5 and 5 μm. These emissions will be observed mainly at the end of the mission, at distances from the Sun of less than 2 AU.
- Identification of the gas molecules. The 2–5 μm range corresponds to the maximum efficiency of molecular

resonant fluorescence at fundamental rotational/vibrational bands. A major objective is to identify the hydrocarbon emission in the 3–4 μm range. Such identification requires a resolving power of the order of 2000 at 3.5 μm.
- Assessment of the coma thermodynamics. Determine and map the rotational temperatures for the individual lines of H_2O with an accuracy of 1 K and a nominal S/N of 200.
- Detection of early gaseous activity. Spectra will be obtained at long integration times, starting before the mapping phase, to search for CO emission as an indicator of beginning activity.
- Determination of *ortho*/*para* ratio for H_2O. Long integration should allow a determination of the OPR with a S/N ratio of 50 to discriminate among different scenarios of comet formation.
- Determination of isotopic ratios for selected molecules, such as ^{13}CO, $H_2\,^{17}O$, $H_2\,^{18}O$ or HDO.

Asteroids

- Determination of the spatial distribution of the various mineralogical types and their mixtures.
- Construction of albedo maps.
- Determination of the existence of possible asteroids satellites (in the NIR).

Technical description

VIRTIS instrument is part of the ROSETTA orbiter payload. It is a visible and infrared imaging spectrometer designed to fulfil the objectives of the VIRSTM model payload instrument and to take into account the mission scenario. In order to fully achieve these objectives, the VIRTIS instrument performances have to exceed the specifications of the baseline model payload instrument (Bar-Nun *et al.*, 1993). The VIRTIS instrument combines a double capability: (1) high-resolution visible and infrared imaging in the 0.25–5 μm range at moderate spectral resolution (VIRTIS-M channel) and (2) high-resolution spectroscopy in the 2–5 μm range (VIRTIS-H channel). This improved capability considerably enlarges the scientific return of the instrument. The two channels will observe the same comet areas in combined modes to take full advantage of their complementarities. VIRTIS-M (named -M in the following) is characterised by a single optical head consisting of a Shafer telescope combined with an Offner imaging spectrometer and by two bidimensional FPAs: the VIS (0.25–1 μm) and IR (1–5 μm). VIRTIS-H (-H) is a high-resolution infrared cross-dispersed spectrometer using a prism and a grating. The 2–5 μm spectrum is dispersed in 10 orders on a focal-plane detector array.

General instrument description

VIRTIS is a sophisticated imaging spectrometer that combines three unique data channels in one compact instrument. Two of the data channels are devoted to spectral mapping and are housed in the Mapper (-M) optical subsystem. The third channel is devoted solely to spectroscopy and is housed in the high resolution (-H) optical subsystem. The addition of the -H subsystem makes VIRTIS increase by more than 30% the scientific yield of the ROSETTA Model Payload instrument, the "VIS and IR Mapping Spectrometer", while maintaining the same mass allocation (Reininger *et al.*, 1996).

As shown in the functional block diagram of Fig. 4 and -M and -H optical subsystems are housed inside the Cold Box of the Optics Module. -M utilises a silicon charge coupled device (CCD) to image from 0.25 μm to 1 μm and a mercury cadmium telluride infrared focal plane array (IRFPA) to image from 1 to 5 μm. -H requires a similar HgCdTe IRFPA to perform spectroscopy from 2 to 5 μm. The Proximity Electronics to drive the CCD and the two IRFPAs are housed inside the Pallet of the Optics Module, and the remaining electronics cards are housed inside the Main Electronics Module. Both IRFPAs require active cooling to minimise the detector dark current (thermally generated Johnson noise).

The VIRTIS design has already been refined in order to reduce its total mass without relying on sophisticated materials or electronics packaging and without degrading its scientific performance. The total mass of VIRTIS is now of 23 kg.

Optics module description. There are two unique optical systems housed in the Optics Module: the -M imaging spectrometer and the -H echelle spectrometer. The -M optical concept is inherited from the visible channel of the Cassini Visible Infrared Mapping Spectrometer (VIMS-V) developed at Officine Galileo (Florence). The VIRTIS version of the concept matches a Shafer telescope to an Offner grating spectrometer to disperse a line image across two FPAs. The -H with a quite different function, uses a cross dispersing prism and a flat diffraction grating to lay ten high resolution orders across a FPA. Figure 5 is a scale representation of the two optical systems, as seen from the $-y$ axis for -H and the $+z$ axis for -M. Table 5 lists the instrument optical specifications. The two optical systems compensate for each other in the sense that -M can first map the comet by creating moderately high resolution spectral images and then -H can perform very high resolution spectroscopy on selected zones of interest.

VIRTIS-M. The Shafer telescope is the combination of an inverted Burch telescope and an Offner relay. The Offner relay takes the curved, anastigmatic virtual image of the inverted telescope and makes it flat and real without losing the anastigmatic quality. Coma is eliminated by putting the aperture stop near the center of curvature of the primary mirror and thus making the telescope monocentric. The result is a telescope system that relies only on spherical mirrors, yet remains diffraction limited over an appreciable spectrum and field: at ± 1.8 degrees the spot diameters are less than 6 μm in diameter, which is 7 times smaller than the slit width.

Cassini-VIMS and OMEGA-VIMS both required separately housed co-aligned instruments to cover the visible and infrared spectra. The Offner spectrometer not only does away with redundant optical systems, it eliminates the need for collimators, camera objectives, and beam splitters and thereby simplifies fabrication and minimises

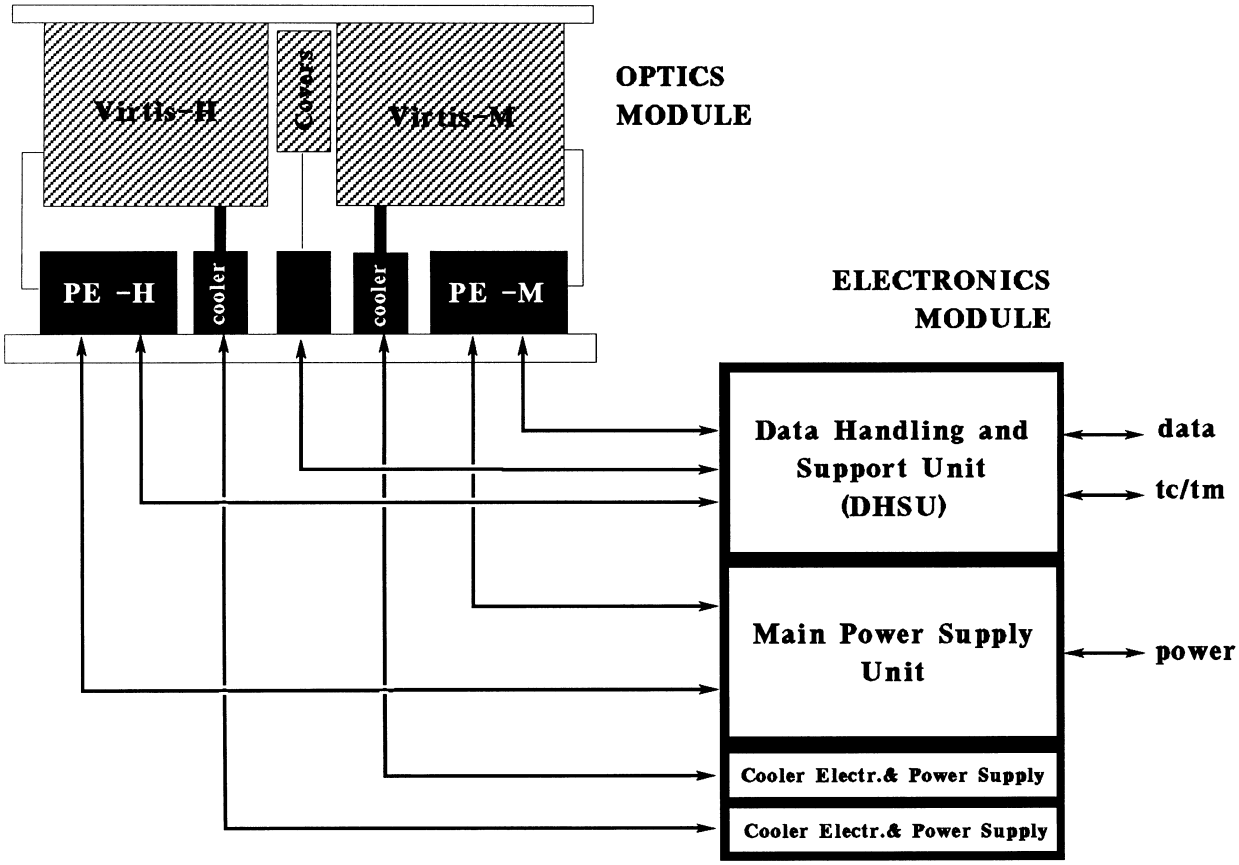

Fig. 4. VIRTIS functional block diagram

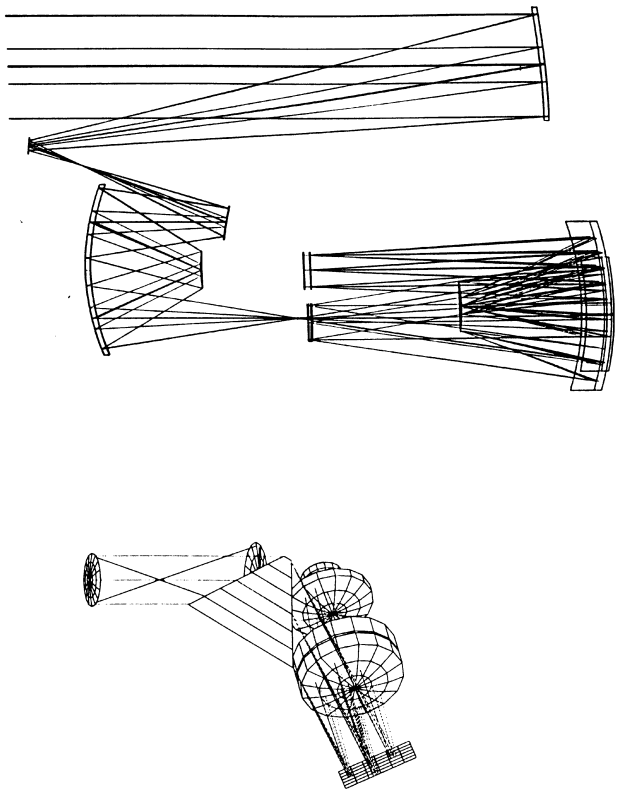

Fig. 5. VIRTIS optical system

volume and mass. However, a grating spectrometer that does not rely on a collimator and camera objective requires perfect mating to its collecting telescope.

The -M spectrometer does not need the beam splitter, but recognises two different groove densities on a single grading substrate. The grating profiles are holographically recorded into a photoresist and then etched with an ion beam. Using various masks the grating surface can be separated into different zones with different groove densities and different groove depths as shown in Fig. 6. The VIS regions, which make up the central 30% of the conjugate pupil area, correspond to the higher groove density for generating the higher spectral resolution required in the "visible" channel extending from the ultraviolet to the near infrared. The smaller pupil area allows the visible channel to operate partially coherently and achieve a smaller point spread function. It should now be obvious that an on-axis telescope cannot be used with this grating concept because the visible portion of the conjugate grating surface would be obscured by the secondary mirror of the telescope.

The reflected infrared solar irradiance is quite low and is not adequately compensated for by the infrared emissions of the cold comet. The infrared channel therefore requires a greater pupil area, about 70% as indicated by the IR region shown in Fig. 6. Since the infrared channel does not require as high a resolution as the visible channel, the lower MTF, caused by the visible zone's obscuration

Table 5. Optics specifications

	VIRTIS-M	VIRTIS-H
Pupil diameter (mm)	50	36
Imaging F/#	5.8 Vis and 3.2 IR	1.67
Etendue (m^2-sr)	3.7×10^{-11} Vis and 8.6×10^{-11} IR	1×10^{-9}
Slit dimension	40 μm $\times$ 10 mm	28 μm $\times$ 142 μm
Spectrometer magnification	1	1.05
MTF at Nyquist (1 mrad)	50%	N/A
FWHM (LSF*slit*pixel)	<40 μm	<40 μm
In field stray light	$<5\%$	$<5\%$
Out of field stray light	$<0.1\%$	$<0.1\%$

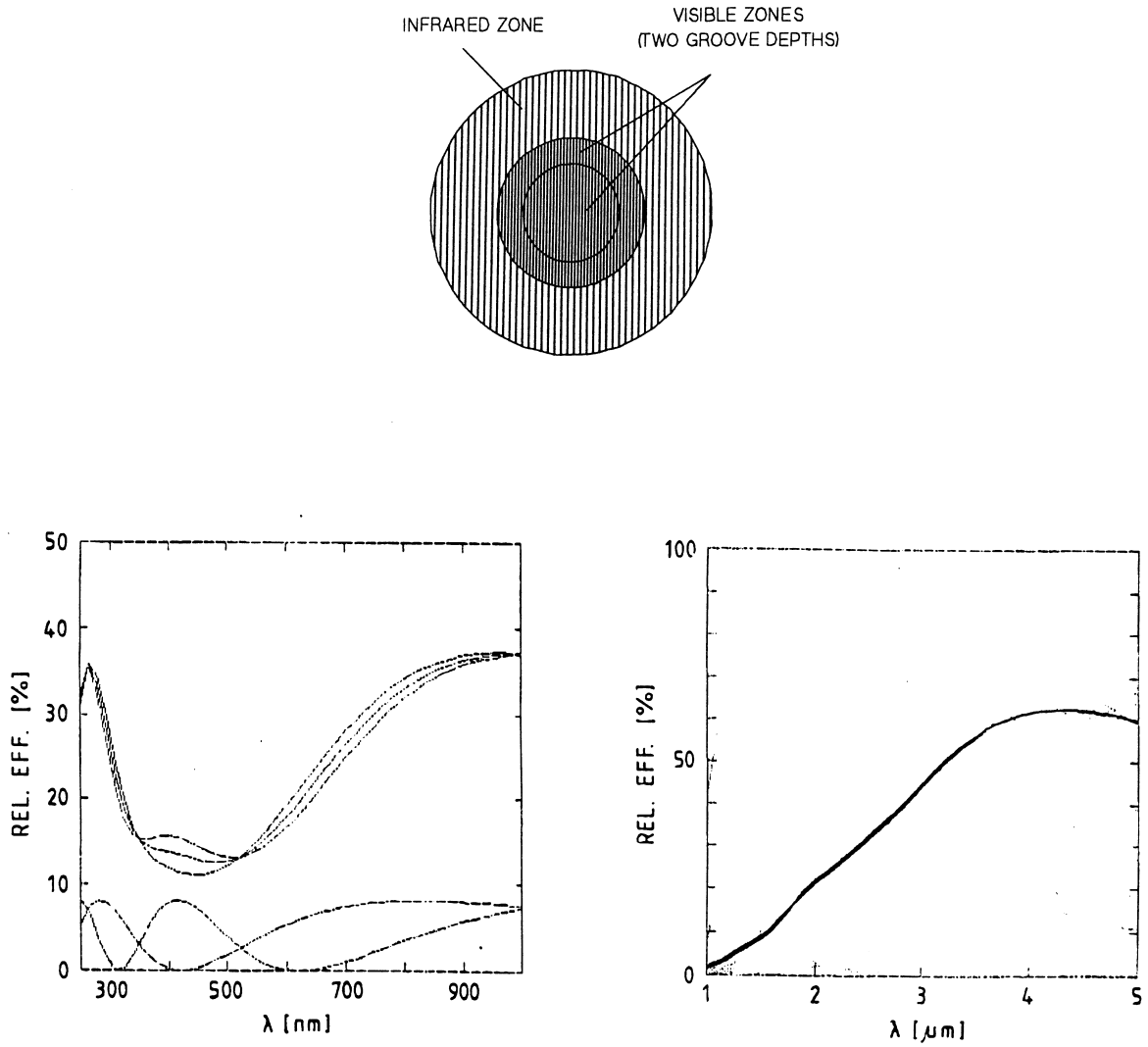

Fig. 6. Top: VIRTIS-M grating zones; bottom: VIRTIS-M grating efficiencies

of the infrared pupil, is acceptable. In any case, the spot diagrams for all visible and infrared wavelengths at all field positions are within the dimension of a 40 μm pixel.

A laminar grating with a rectangular groove profile is used for the visible channel's pupil zone to enable two different groove depths to alter the grating efficiency spectrum and compensate for the low solar energy and low CCD quantum efficiency in the ultra-violet and near infrared regions. The resulting efficiency, shown in Fig. 6, improves the instrument's dynamic range by increasing the S/N at the extreme wavelengths and preventing saturation in the central wavelengths. For the infrared zones, a blazed groove profile is used that results in a peak efficiency at 5 μm to compensate for the low signal levels expected at this wavelength.

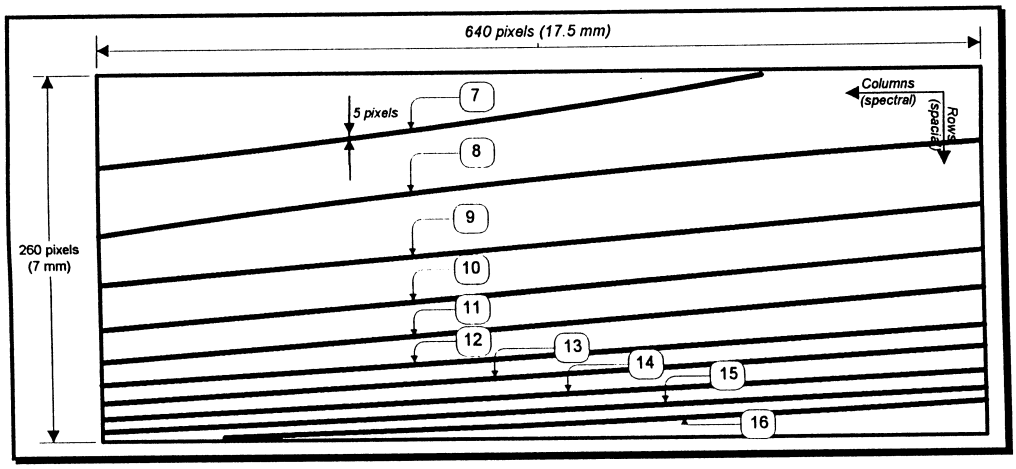

Fig. 7. Sensitive surface of the 640×260 VIRTIS-H IRFPA, showing the spatial distribution of the spectral orders 7–16

VIRTIS-H. In -H the light is collected by an off-axis parabola and then collimated by another off-axis parabola before entering a cross-dispersing prism made of lithium fluoride. After exiting the prism, the light is diffracted by a flat reflection grating which disperses it in a direction perpendicular to the prism dispersion. The prism allows the low groove density grating, which is the echelle element of the spectrometer, to achieve very high spectral resolution by separating orders 7 through 16 across a two-dimensional detector array as shown in Fig. 7. The spectral resolution varies in each order between 1200 and 3500.

Since the -H is not an imaging channel, it is only required to achieve good optical performance at the zero field position. The focal length of the objective is set by the required IFOV and the number of pixels allowed for summing. While the telescope is F/1.6, the objective is F/1.67 and requires five pixels to be summed in the spatial direction to achieve a 1 mrad^2 IFOV (5×0.45 mrad $\times 0.45$ mrad).

Focal plane arrays. The CCD in -M will be a frame transfer device. Although the device will be so cold that dark current will be negligible, it can be operated at multi-pinned-phase (MPP) to reduce the dark current at room temperature; running the CCD in the inverted mode also limits the damaging effects of radiation. The challenge for -M is to keep the CCD temperature above 155 K to prevent degradation of the charge transfer efficiency (CTE). The 75 K IRFPA will be only 9 mm away so both detector arrays will have adjacent edges free of bond wires. An attempt will be made to eliminate the filter window and associated package by putting the filters directly on the detectors. This will also eliminate ghost images caused by multiple reflections.

A chrome-gold thin film on the front surface of the CCD is used to improve the capture cross-section of the long wavelength photons, while lumogen coating is used to enhance the efficiency in the UV range. The CCD specifications are listed in Table 6.

The baseline for both the -M and -H IRFPAs are mercury cadmium tellluride on sapphire substrates. The -M and -H detectors have the same 5.1 μm cut-off wavelength requirement and can therefore be manufactured from the same wafers. To reduce dark current the -M IRFPA must be cooled to below 70 K. Passive cooling has been rejected because the low emissive power of passive radiators and the risk of comet contamination indicate a minimum radiator area larger than one square metre. Cryocoolers are suitable for the VIRTIS FPA cooling task.

Thermomechanical design concept. Figure 8 is a representation of the thermomechanical concept for the VIRTIS Optical Module, as seen looking from the $+x$

Table 6. FPA specifications

	VIRTIS-M CCD	VIRTIS-M IRFPA	VIRTIS-H IRFPA
Material	Silicon + UV coating	HgCdTe on AlO_2 or CdZnTe	HgCdTe on AlO_2 or CdZnTe
Pixel pitch	38 μm	38 μm	38 μm
Format	256×388	256×412	240×640
Pixel summing	yes—variable	by 2 only	by 2 only
Correlated Double Sampling	off-chip	on-chip	off-chip
Readout	SFD	BDI	BDI
Noise (rms e^-)	<20	280	280
Full well capacity (e^-)	10^6	1.6×10^7	7×10^6
Temperature (K)	155	75 or 90	70 or 85
Dark current (e/s)	<1	72,000	18,000

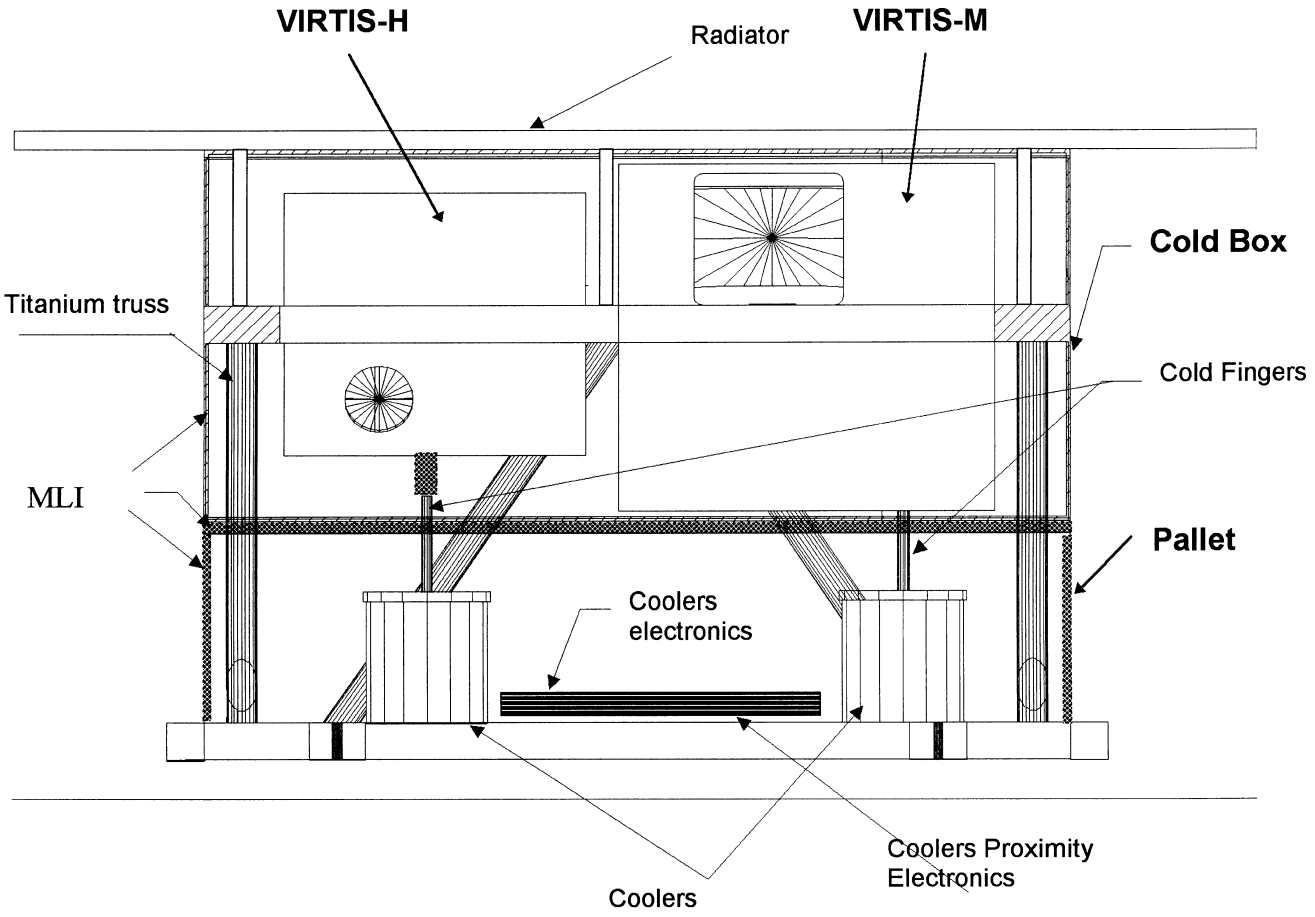

Fig. 8. Optics module mechanical layout

direction. The mechanical interface with the spacecraft is the Pallet baseplate, placed at the bottom of the figure, via eight mounting feet (two per side) on a 450 mm × 510 mm base plate. The Pallet is a hollow box 130 mm high with the coolers and Proximity Electronics mounted inside. The Pallet must dissipate 15 W of which 13 W are expected to be conducted to the spacecraft for radiative dissipation at 300 K. The remaining 2 W are radiated directly by the instrument at lower temperatures.

The Cold Box surface adjacent to the Pallet is covered by multilayer insulation which also covers at least three of the remaining surfaces. A conservative assumption is made that much of the thermal field of view of these surfaces is of high emissivity parts of the spacecraft.

The low conductive heat load will be achieved by mounting the Cold Box on 8 struts, on which number and attachment positions were selected to avoid distortion upon cooling from room temperature.

The empty space in the Cold Box is intentional, to allow enough radiating surface area, without requiring a separate and complex radiator. The result is a low density module with stiffness structures only where necessary. This reduces mass while maintaining the surface area. Irregular shapes were eliminated to facilitate efficient MLI attachment.

Main electronics module

The main electronics are physically separated from the optics module. The Electronics Module houses the power supply for the whole of the experiment; the cooler electronics; the Spacecraft interface electronics, for telemetry and telecommanding; the interfaces with the Optics Module subsystems; and the DHSU (Data Handling and Support Unit), which is the electronics for the data handling, processing and for the instrument control.

The data processing and the data handling activities in the DHSU will be performed using the on-line philosophy. The data will be processed and transferred to the spacecraft in real time. The mass memory (SSR) of the spacecraft will be used to store or buffer a large data volume. The main electronics contains no additional hardware component for data processing and compression. All data processing will be performed by software.

Virtis observation strategy

The ROSETTA mission is characterised by different mission phases. In what follows we have summarised the

scientific objectives in these phases. During the six cruise phases VIRTIS will be generally switched off, as in other experiments, with the exclusion of periodical testing of VIRTIS and calibration sessions including Sun calibrations through the Solar calibration units (before any main event).

Due to the high relative velocity in the Mars fly-by, observations of the atmosphere at Mars will be performed by VIRTIS, from a great distance. The importance of this phase cannot allow observations in close proximity. However observations performed at distance will be scientifically valuable.

The candidate asteroid for the first fly by will be Mimistrobell. Mimistrobell will be detected at about 1,700,000 km, at 5 μm with an integration time of 4 s. The maximum spatial resolution is about 100 m/pixel. During the approach phase albedo measurements in the VIS and IR will be taken. The second asteroid—possibly Rodari—encounter geometry is not known well enough to permit evaluation of data volume. The asteroid fly-bys will allow multispectral imaging of the surface in order to identify their mineralogical composition.

During the approach, we assume that the measurements will start when the asteroid fills a pixel. In this case the time between the first acquisition and the last possible measurement is about 3 h. In this phase we expect to pick up the comet for the first time at a distance depending on the albedo and the temperature of the object. For a 10-s integration time the comet will be detected at a distance of 70,000 km to 40,000 km depending on the wavelength selected for the observation. As soon as the comet is picked up, the spectral phase curve can be performed. This will be important in order to create a reference case to be compared with the ground-based observations. As far as -H is concerned we foresee one observation per day using a long integration time in order to search for early comet emissions (CO and H_2O).

The comet-mapping phase will begin when the spacecraft starts orbiting around the comet at 3.2 AU. It is estimated that this phase will last 70 days for mapping and a further 30 days for planning purposes. We have developed an orbital simulator to choose the optimal orbits for mapping purposes. For the simulations a triaxial ellipsoid of mean radius 0.6 km with axes in the relative proportions 1:0.7:0.5 will be used as a standard model of the nucleus. The rotational period has been assumed to be 6 h. In the numerical simulation 500 mass points have approximated the nucleus with random deformations in density and surface shape. For a typical elliptical quasi polar orbit, (with periaster at 5 comet radii and apoaster at 25 comet radii, tilted in such a way as to guarantee that the instrument axes will not look in the direction of the Sun, and for an inclination of the comet rotation axis of 30°) the time taken to cover 80% of the nucleus surface will be about 10 days with a typical space resolution of 12 m for the mapper and a dwell time of 60 s. By dwell time we mean the residence time of the spot of the nucleus surface in the IFOV of the two channels. The results discussed above for the surface coverage depend strongly on the comet rotation period. The longer the period the longer the time needed to map the surface.

In the Closest Approach phase combined observations of -H and -M will be required in order to select the most scientifically valuable landing sites.

For Coma observation a minimum distance to the nucleus of the order of 100 km is required. For cartography of the coma, observations at several phase angles are needed to retrieve the spatial distribution and the morphology of the coma. Long integration times also are needed to obtain spectra of minor constituents. Assuming 8 months of observations, we foresee high-resolution observations with -H and -H observations combined with -M for coma mapping. Coma mapping is also of interest for MIRO experiment, and a common observing strategy will be fruitful. A requirement for VIRTIS coma mapping will be to scan in two orthogonal directions.

If the instrument survives the perihelion passage, search for variations of the nucleus following onset of coma activity will be performed. Mapping of active and inactive regions will give a new insight of the development and decline of comet activity.

Concluding remarks

From the previous discussion it is apparent that the VIRTIS experiment will allow us to acquire a new knowledge of the minor bodies physics and chemistry as well a knowledge of the complex relationships between comets and asteroids. The Cassini inheritance has been particularly valuable in designing the VIRTIS instrument. We expect to achieve with the ROSETTA mission not only new scientific results but also to build up in Europe a more experienced and efficient planetology community.

References

A'Hearn, M. F., Millis, R. L., Schleicher, D. G., Osip, D. J. and Birch, P. V. (1997) The ensemble properties of comets: results from narrowband photometery of 85 comets, 1976–1992. *Icarus*, in press.

Bar-Nun, A., Barucci, A., Bussoletti, E., Coradini, A., Coradini, M., Colangeli, L., Eberhardt, P., Grün, E., Hechler, M., Keller, U., Kissel, J., Klinger, J., Langevin, Y., Laurance, R. J., McDonnell, J. A. M., Milani, A., Picardi, G., Pillinger, C., Schwehm, G., Stöffler, D. and Wänke, H. (1993) ROSETTA Comet Rendezvous Mission. ESA Report, SCI(93)7.

Benkhoff, J. and Boice, D. C. (1996) Modelling the thermal properties of the gas flux from a porous, ice-dust body in the orbit of P/Wirtanen. *Planet Space Sci.* **44,** 665–673.

Bocklee-Morvan, D. and Crovisier, J. (1992) The formation and composition of the atmospheres of small solar system bodies. In: *Proceedings of the* 30*th Liege Int. Astr. Coll.* 65–82.

Brooke, T. Y., Tokunaga, A. T., Weaver, H. A., Crovisier, J., Bockelee-Morvan, D. and Crisp, D. (1996) Detection of acetylene in the infrared spectrum of comet Hyakutake. *Nature* **383,** 606–608.

Capria, M. T., Capaccioni, F., Coradini, A., De Sanctis, M. C., Espinasse, S., Federico, C., Orosei, R. and Salomone, M. (1996) A P/Wirtanen evolution model. *Planet. Space Sci.* **44,** 987–1000.

Carusi, A., Kresak, L. and Valsecchi, G. B. (1995) Electronic atlas of evolution of short-period comets, on line: http://titan.ias.fra.cnr.it/ias-home/ias-home.html.

Clark, R. N. (1981) Water frost and ice: the near infrared spectral reflectance 0.65–2.5 m. *J. Geophys Res.* **86-B4,** 3087.

Combes, M., Moroz, V. I., Crovisier, J., Encrenaz, T., Bibring,

J. P., Grigoriev, A. V., Sanko, N. F., Coron, N., Crifo, J. F., Gispert, R., Bockelee-Morvan, D., Nikolsky, Y. V., Kransnopolsky, V. A., Owen, T., Emerich, C., Lamarre, J. M. and Rocard, F. (1986) The 2.5–12 micron spectrum of Halley from the IKS Vega experiment. *Icarus* **76,** 404–436.

Coradini, A., Capaccioni, F., Capria, M. T., De Sanctis, M. C., Espinasse, S., Orosei, R., Salmone, M. and Federico, C. (1997a) Transition elements between comets and asteroids: evolutionary models. Part I. *Icarus* (in press).

Coradini, A., Capaccioni, F., Capria, M. T., De Sanctis, M. C., Espinasse, S., Orosei, R., Salmone, M. and Federico, C. (1997b) Transition elements between comets and asteroids: From the Kuiper belt to NEOs, Part II. *Icarus* (in press).

Crovisier, J., Brooke, T. Y., Hanner, M. S., Keller, H. U., Lamy, P. L., Altieri, B., Bockelee-Morvan, D., Jorda, L., Leech, K. and Lellouch, E. (1996) The infrared spectrum of comet C/1995 O1 (Hale-Bopp) at 4.6 AU from the Sun. *Astron. Astrophys.*, **315,** 385–388.

Crovisier, J., Leech, K., Bockelee-Morvan, D., Brooke, T. Y., Hanner, M. S., Altieri, B., Keller, P. L. and Lellouch, E. (1997) The spectrum of comet C/1995 O1 (Hale Bopp) observed with the Infrared Space Observatory at 2.9 AU from the Sun. *Science* **275,** 1904.

Farinella, P. and Davis, D. R. (1996) Short period comets: primordial bodies or collisional fragments, *Science* **273,** 938–940.

Festou, M. C., Feldman, P. D., A'Hearn, M. F., Arpigny, C., Cosmovici, C. B., Danks, A. C., McFadden, L. A., Gilmozzi, R., Patriarchi, P., Tozzi, G. P., Wallis, M. K. and Weaver, H. A. (1986) IUE observations of comet Halley during the Vega and Giotto encounters. *Nature* **321,** 361–363.

Haruyama, J., Yamamoto, T., Mizutani, H. and Greenberg, J. M. (1993) Thermal history of comets during residence in the Oort cloud: effect of radiogenic heating in combination with very low thermal conductivity of amorphous ice. *JGR*, **98,** 15,079–15,090.

Jones, T. D., Lebofsky, L. A., Lewis, J. S. and Marley, M. S. (1990) The composition and origin of the C, P, and D asteroids: water as a tracer of thermal evolution in the outer belt. *Icarus*, **88,** 172–192.

Jorda, L. and Rickman, H. (1995) Comet P/Wirtanen, summary of observational data. *Planet. Space Sci.* **43**(3/4), 575–579.

Keller, H. U., Kramm, R. and Thomas, N. (1988) Surface features on the nucleus of comet Halley. *Nature*, **331,** 227–231.

Mumma, M. J., Weaver, H. A. and Larson, H. P. (1987) The ortho-para ratio of water vapour in comet P/Halley. *Astron. Astrophys.* **187,** 419.

Mumma, M. J., DiSanti, M. A., Russo, N. D., Fomenkova, M., Magee-Sauer, K., Kaminski, C. D. and Xie, D. X. (1996) Detection of abundant ethane and methane along with carbon monoxide and water, in comet C/1996 B2 Hyakutake: evidence for interstellar origin. *Science* **272,** 1310.

Podolak. M. and Prialnik, D. (1996) Models of the structure and evolution of comet P/Wirtanen. *Planet. Space Sci.* **44,** 655–664.

Reininger, F. and the VIRTIS team (1996) VIRTIS: Visible Infrared Thermal Imaging Spectrometer for the ROSETTA Mission. *SPIE Imaging Spectrometry II* **2819,** 66–77.

Rickman, H. and Huebner, W. F. (1990) Comet formation and evolution. In *Physics and Chemistry of Comets*, ed. W. F Huebner, pp. 245–303. Springer Verlag.

Schulz, R. and Schwehm, G. (1996) P/Wirtanen: necessary observations in support of ROSETTA. *Planet. Space Sci.* **44,** 619–624.

Singer, R. B. (1981) Near infrared spectra reflectance of mineral mixture: systematic combinations of pyroxenes, olivine, and iron oxides. *J. Geophys. Res.* **86,** 7967.

Wirtanen, C. A. (1948) Comet 1948b. IAUC, 881.